

*To appear in “Extragalactic Gas at Low Redshift”  
 ASP Conference Series, Vol. TBD, 2001  
 ed. J. Mulchaey*

## Phase Structure of Weak MgII Absorbers: Star Forming Pockets Outside of Galaxies

Jane C. Charlton, Christopher W. Churchill, Jie Ding, Stephanie Zonak,  
 Nicholas Bond

*Department of Astronomy and Astrophysics, Penn State, University Park, PA 16802*

Jane R. Rigby

*Astronomy Department, University of Colorado, Campus Box 391, Boulder, CO 80309*

**Abstract.** A new and mysterious class of object has been revealed by the detection of numerous weak MgII doublets in quasar absorption line spectra. The properties of these objects will be reviewed. They are not in close proximity to luminous galaxies, yet they have metallicities close to the solar value; they are likely to be self-enriched. A significant fraction of the weak MgII absorbers are constrained to be less than 10 parsecs in size, yet they present a large cross section for absorption, indicating that there are a million times more of them than there are luminous galaxies. They could be remnants of Population III star clusters or tracers of supernova remnants in a population of “failed dwarf galaxies” expected in cold dark matter structure formation scenarios.

### 1. Introduction

Quasar absorption line systems were once thought to be distinct classes of objects, such as the Ly $\alpha$  forest, CIV systems, or MgII systems. Now it is recognized that there is considerable overlap between these classes. The remaining challenge is to achieve complete understanding of the relationship between the absorption line systems and the gaseous galaxies and intergalactic structures in which they arise.

A clear association has been established between strong MgII absorption lines and relatively luminous galaxies,  $> 0.1L_*$  (eg., Bergeron & Boissé 1991; Steidel, Dickinson, & Persson 1994; Steidel 1995). However, the gaseous structures giving rise to weak MgII absorbers, those with rest frame equivalent widths,  $W_r(2796)$ , less than 0.3 Å have not yet been identified. In this contribution, we use other chemical transitions such as FeII, CIV, SiIV and Ly $\alpha$  to determine if multiple ionization phases of gas are present and to constrain their physical properties. We then speculate about the origin of the weak MgII absorbers.

## 2. Statistics

In Figure 1, we show examples of three single-cloud weak MgII absorbers and one multiple cloud (bottom right panel) weak MgII absorber. At  $0.5 < z < 1.0$ ,

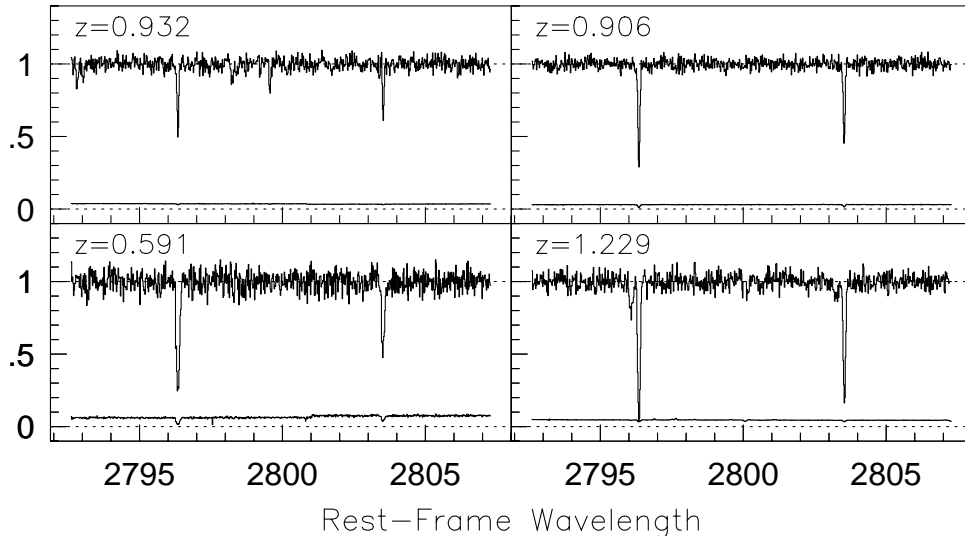


Figure 1. Representative “weak” MgII absorbers as seen in HIRES/Keck spectra (Churchill et al. 1999, ApJS, 120, 51). The MgII  $\lambda\lambda 2796, 2803$  doublet is displayed in the rest frame. The sample includes three single and one double (bottom right panel) component weak absorbers.

weak MgII absorbers are more numerous than strong absorbers. The equivalent width distribution of MgII absorbers is shown in Figure 2. It rises rapidly toward weaker lines, and for  $W_r(2796) < 0.3$  Å, there are  $dN/dz = 1.74 \pm 0.10$  systems per unit redshift. However, some of these systems have multiple clouds and are kinematically similar to stronger MgII systems. Considering only the single-cloud weak MgII absorbers, we find  $dN/dz = 1.16 \pm 0.07$ .

## 3. Comparing MgII, FeII, CIV, and HI Absorption

Clues to the nature of single-cloud weak MgII absorbers are derived from a comparison of other transitions detected at the same velocity. Figure 3 shows, for 15 systems, the regions of the observed spectrum in which the key transitions, FeII, CIV, and Ly $\alpha$ , as well as the Lyman limit, would appear given the presence of weak MgII. The MgII and FeII absorption profiles were obtained with a resolution of  $\sim 6$  km s $^{-1}$  with HIRES/Keck (see Churchill et al. 1999). The CIV, Ly $\alpha$ , and Lyman series coverage, with resolution 230 km s $^{-1}$ , was obtained with the Faint Object Spectrograph (FOS) aboard the *Hubble Space Telescope* (HST), primarily as part of the HST QSO Absorption Lines Key Project (Bahcall et al. 1993; Bahcall et al. 1996; Jannuzi et al. 1998).

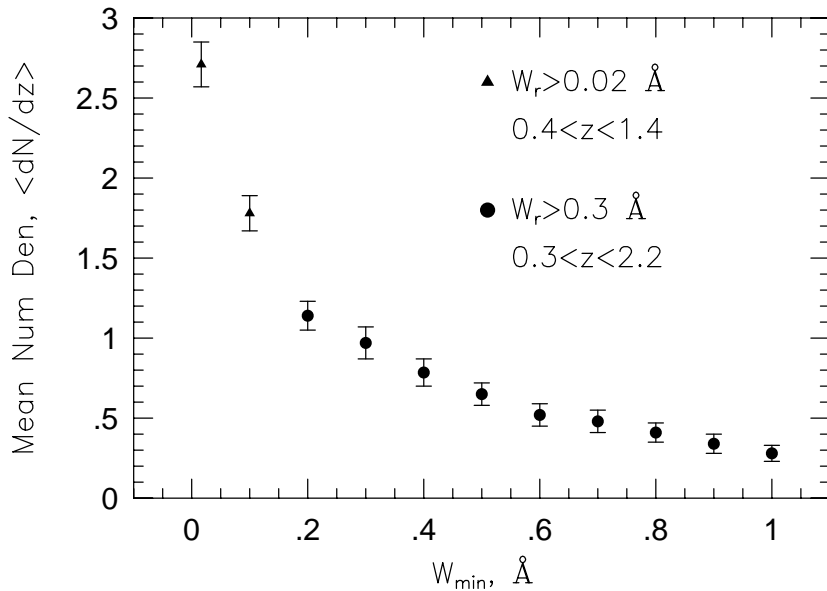


Figure 2. The number density of absorbers with equivalent widths,  $W$ , greater than a well-defined minimum,  $W_{min}$ , measured over finite redshift bins. The data for weak MgII absorbers are taken from Churchill et al. (1999), and those for strong MgII absorbers from Steidel and Sargent (1992).

In Figure 3, three of the 15 systems, labeled S7, S13, and S18, have detected FeII with a column density comparable to MgII. For these iron-rich single-cloud weak MgII systems,  $dN/dz \simeq 0.18$ . Seven of the 15 systems are constrained to have multiphase conditions. For five of those (S7, S17, S19, S20, and S28), the CIV is too strong to arise in the same phase with the MgII. For three systems (S3, S15, and S20), the HI cannot be produced in the same phase with the MgII. This is discussed in detail by Rigby, Charlton, and Churchill (2001) and the key points are summarized below.

#### 4. Physical Conditions for Single-Cloud Weak MgII Absorbers

##### 4.1. From Photoionization Models

The photoionization code Cloudy (Ferland 1996) was used to infer the metallicity and ionization condition in weak MgII absorbers. Cloudy calculated the densities of the different ions for various chemical elements, layer by layer, as incident photons traveled through a slab of material. The input parameters for Cloudy were the metallicity and the ionization parameter (ratio of the number density of photons to the number density of electrons). We assumed the ionizing radiation spectrum from the extragalactic background was the modified quasar spectrum of Haardt and Madau (1996). Since the photon number density is set, the ionization parameter translates directly to an electron number density.

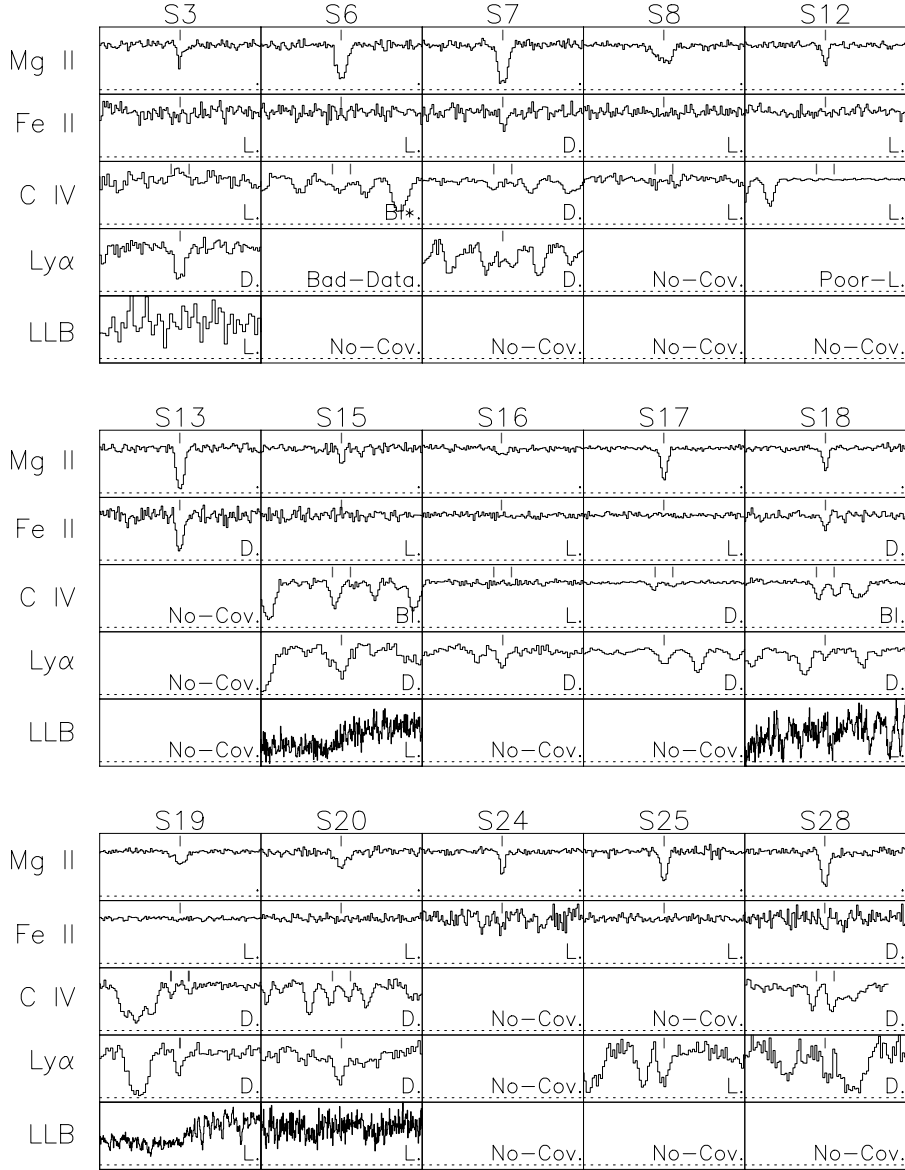


Figure 3. The “data matrix” for the single-cloud weak MgII systems. For each absorber, the MgII  $\lambda 2796$  transition is shown in the top sub-panel. In the lower sub-panels, we present the spectral regions where the FeII  $\lambda 2600$  (or  $\lambda 2383$ ) transition, the CIV doublet, the Ly $\alpha$  transition, and the Lyman limit break are expected. Ticks above the spectra give the locations where features are expected. The full velocity window of the sub-panels with MgII and FeII from HIRES/Keck is  $100 \text{ km s}^{-1}$  and for the FOS/HST data is  $5000 \text{ km s}^{-1}$ . “No-Cov” indicates that the spectral region was not observed, and “Bad-Data” indicates that signal-to-noise ratio in the spectral region was too low for a useful measurement. “D” indicates a clean detection at the  $3\sigma$  or greater significance level. “L” denotes no detection, but only an upper limit on the equivalent width. “Bl” indicates poor constraints due to blending with other features. Transitions not plotted can be found in Churchill et al. (2000).

Figure 4 summarizes the dependence of ratios of the constraining transitions,  $N(\text{FeII})/N(\text{MgII})$  and  $N(\text{CIV})/N(\text{MgII})$ , on ionization parameter,  $\log U$ . In the optically thin regime, this is virtually independent of metallicity because all layers of the slab are exposed to the same radiation.

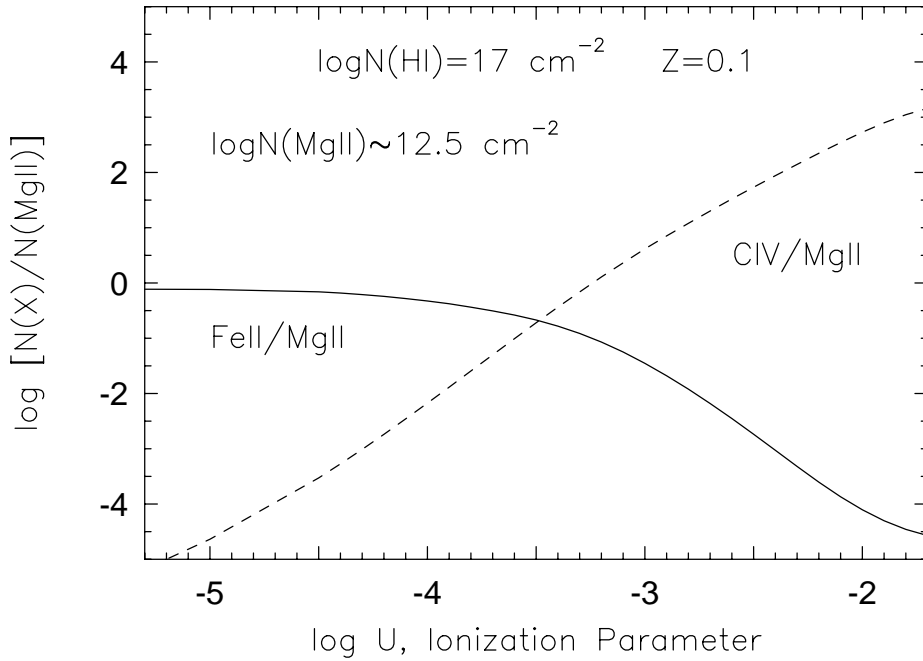


Figure 4. The ratios  $N(\text{FeII})/N(\text{MgII})$  and  $N(\text{CIV})/N(\text{MgII})$  are uniquely determined functions of the ionization parameter over three orders of magnitude in  $\log U$ . Since ionization structure is not important for weak MgII absorbers, the ratios are independent of metallicity. Note that at low values of  $\log U$ , the FeII/MgII ratio flattens and thus provides less constraint.

The ratio  $N(\text{FeII})/N(\text{MgII})$  is quite sensitive to  $\log U$  for  $\log U > -3.5$ , but it flattens and does not provide a good constraint for lower values of  $\log U$ . For the three iron-rich systems shown in Figure 3,  $N(\text{FeII})/N(\text{MgII})$  is close to one so that  $\log U < -3.5$ , and therefore electron number density  $\log n_e > 0.01 \text{ cm}^{-3}$  applies. In these weak MgII absorbers, the total column density is relatively small, and the high density translates to a thickness of less than 10 pc.

$N(\text{CIV})/N(\text{MgII})$  also provides a strong constraint on the ionization parameter. For some systems, the observed ratio is so large that multiphase conditions are required (S7, S17, S19, S20, and S28 in Figure 3).

For almost all single-cloud weak systems for which there is a constraint, the metallicities are greater than 0.1 solar, and in many cases close to solar. This constraint comes from a Ly $\alpha$  line, which is weak compared to the MgII, and/or from the absence of a Lyman limit break.

#### 4.2. The Story of Three Single-Cloud Weak MgII Absorbers

For three single-cloud weak MgII absorbers along the line of sight toward the quasar PG 1634 + 706, observations were obtained at high resolution ( $R = 30,000$ ) with the Space Telescope Imaging Spectrograph (STIS) aboard HST. The key transitions for these three systems are compared in Figure 5. None of these three systems classify as iron-rich, because they do not have detected FeII. Methods of modeling these three systems, and details of the results, are described in Charlton et al. (2001). A brief summary follows.

In the  $z = 0.8182$  system, the CIV absorption requires a second broader phase ( $b \simeq 10 \text{ km s}^{-1}$ ) centered at the same velocity as the phase that produces the weak MgII absorption (with  $b \simeq 2 \text{ km s}^{-1}$ ). The relatively weak Ly $\alpha$  constrains the system to have solar metallicity. The low ionization phase has a relatively high density,  $\sim 0.1 \text{ cm}^{-3}$ , and therefore a small size (parsec scale). The high ionization phase is hundreds of parsecs in size, as constrained by SiIV and Nv, as well as CIV. The simplest physical interpretation of these results is a small dense region embedded in a larger more diffuse region. However, in a photoionized model the phases are not in pressure balance because their temperatures are nearly equal.

In the  $z = 0.9056$  system, the CIV is stronger than in the  $z = 0.8182$  system. The metallicity is constrained to be solar or higher. It requires a separate higher ionization phase centered on the MgII, but it also shows an asymmetric structure indicating that an additional cloud  $\sim 13 \text{ km s}^{-1}$  to the red is required. For this system, the low ionization phase is of lower density,  $\sim 0.01 \text{ cm}^{-3}$ , than in the  $z = 0.8182$  system, and its size is 30 to 100 pc. The high ionization phase is somewhat larger. Physically, the lower ionization phase could be embedded within the higher ionization phase, or the high ionization gas could be in the interior of a cold shell (fragmented so that we do not see two cold components from opposite sides of the shell). The additional cloud could arise from gas physically separated from the other material.

The  $z = 0.6564$  system has considerably stronger Ly $\alpha$  absorption than the other two systems, indicating a lower metallicity of less than a tenth solar. This appears to be quite unusual since most single-cloud weak MgII absorbers have close to solar metallicity. The CIV in this system has complex structure, with two offset clouds (at  $24$  and  $54 \text{ km s}^{-1}$ ) that are more highly ionized and do not give rise to MgII absorption. The absorption profiles at the position of the MgII cloud are best fit with two phases, because the CIV profiles is broad relative to the MgII.

#### 4.3. Comparison to the Ly $\alpha$ Forest

The single-cloud weak MgII absorbers are mostly sub-Lyman limit systems, with  $\log N(\text{H}_1) < 16.8 \text{ cm}^{-2}$ . This is shown statistically in the left hand panel of Figure 6. The number of strong MgII absorbers is comparable to the number of Lyman limit systems, which implies that nearly all strong MgII absorbers give rise to a Lyman limit break (Churchill et al. 2000). The number of weak MgII absorbers (two-thirds of which are single-cloud systems) exceeds the number of Lyman limit systems by a factor of two. Therefore, statistically, the vast majority of weak MgII absorbers must not give rise to a Lyman limit break. This is confirmed in the right hand panel of Figure 6, which shows that all the

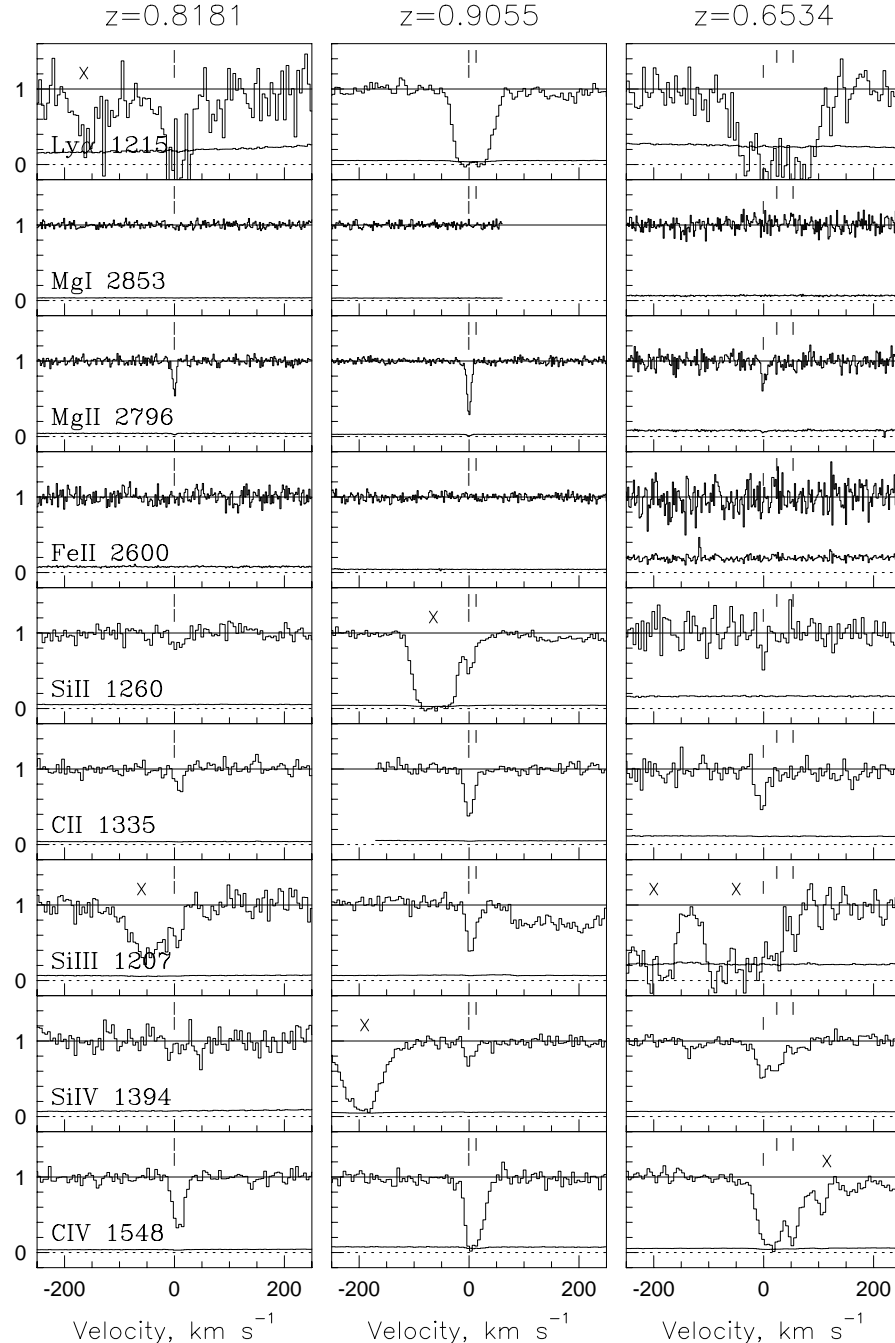


Figure 5. Comparison plot of key transitions for the three weak, single-cloud MgII absorbers along the PG 1634 + 706 line of sight. Detected transitions and constraining limits are presented in velocity space. The data are at  $R = 45,000$  from HIRES/Keck for the MgII, MgI, and FeII transitions. All other transitions are taken from STIS/HST spectra (combining observations by P.I.'s Scott Burles and Buell Jannuzzi), at resolution  $R = 30,000$ . The position of the lower row of ticks, displayed above all of the transitions (at zero velocity), was determined based upon a simultaneous Voigt profile fit to the MgII doublet. The upper row of ticks show velocities of the additional components that were required to fit CIV.

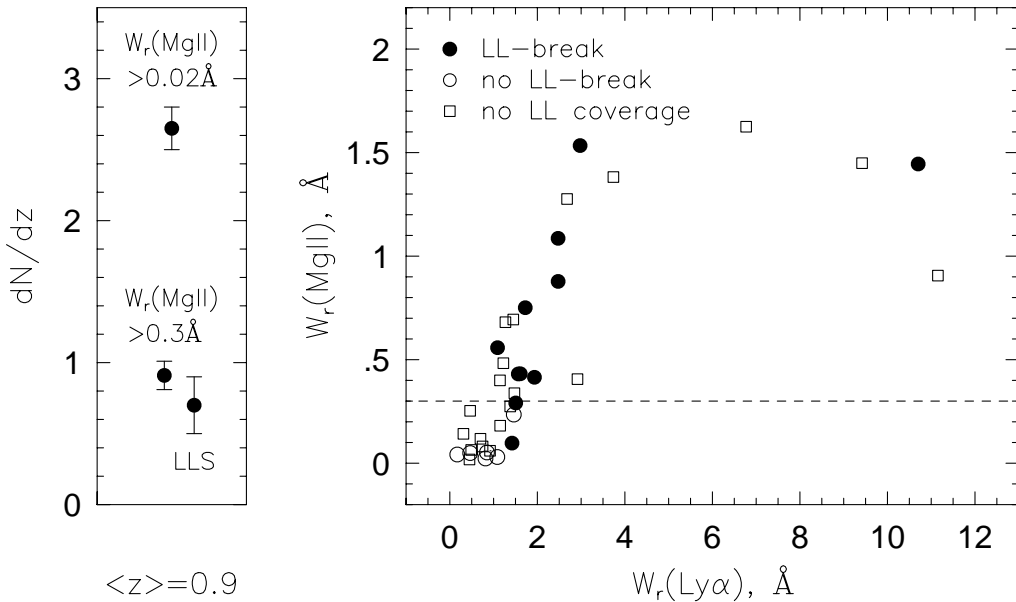


Figure 6. (left)- The redshift number density of Lyman limit systems (LLSs), strong Mg II systems, and all Mg II systems including weak systems. Taken from Churchill et al. (1999). (right)- The Mg II - Ly  $\alpha$  equivalent width plane showing the optically thick (solid circles) and optically thin (open circles) systems. Systems for which no Lyman limit coverage is available are shown as open squares. The dotted line marks the boundary between strong and weak Mg II absorbers. Taken from Churchill et al. (2000).

strong Mg II absorbers for which data were available are found to have Lyman limit breaks. All but one of the weak Mg II absorbers are found not to have Lyman limit breaks.

Most all single-cloud weak Mg II absorbers are Ly  $\alpha$  forest clouds in the sense that their neutral hydrogen column densities are  $< 10^{16.8} \text{ cm}^{-2}$ . We have discussed above that they usually have metallicities close to solar. By number, they comprise between 25 and 100% of the Ly  $\alpha$  forest with  $15.8 < \log N(\text{H I}) < 16.8 \text{ cm}^{-2}$  (Rigby et al. 2001). Weak Mg II absorbers could arise in Ly  $\alpha$  clouds with still smaller  $N(\text{H I})$ , but this would require super-solar metallicities. Despite the high metallicities, most of the single-cloud weak Mg II absorbers are not within 50 kpc of high luminosity ( $> 0.05L^*$ ) galaxies. We conclude that a significant portion of the Ly  $\alpha$  forest must be significantly metal enriched by redshift 0.5 to 1.0.

## 5. Surprising Consequences

We now focus on the subclass of iron-rich single-cloud weak Mg II absorbers. Consider the following facts:

- $dN/dz = 0.18$  for the subclass of iron-rich, single-cloud weak MgII absorbers.
- The inferred thicknesses of these objects are  $\sim 10$  pc.
- $dN/dz = 0.91$  for strong MgII absorbers which arise in the regions within  $\sim 40$  kpc of luminous galaxies ( $> 0.05L^*$ ).

Combining these three facts leads to the conclusion that the structures that produce single-cloud weak MgII absorption outnumber the luminous galaxies by factor of more than one million. Also, recall that although that there is no evidence they are near luminous galaxies, the iron-rich, single-cloud weak MgII absorbers are of solar metallicity and they are not  $\alpha$ -element enhanced. *In situ* enrichment by Type Ia supernovae is implied. It could occur within supernova remnants in intergalactic star clusters, perhaps even the elusive Population III, or within an abundant class of invisible dwarf galaxies.

## 6. What are the single-cloud weak MgII absorbers?

From our analysis, we infer the following:

1. The single-cloud weak MgII absorbers are a variety of metal-rich regions in some of the same clouds that produce Ly $\alpha$  forest lines.
2. Their MgII absorption lines are weak primarily because of a lower total hydrogen column density and a higher ionization of the MgII phase, not because of a lower metallicity.
3. The iron-rich absorbers could be gas in star clusters or remnants of Type Ia supernovae. Multiphase structure (a few km/s component and a ten km/s component) suggests that these might arise in larger dark matter halos.
4. These objects could be related to Pop III star clusters (but not globulars because their low-redshift counterparts would easily be detected in the Local Group) or to a population of failed dwarf galaxies expected in CDM models.
5. Weak MgII absorbers without detected FeII may be related to Type II supernova fragments or may be a type of intragroup HVCs. However, as sub-Lyman limit systems they cannot be the same systems detected as HVCs by 21-cm surveys.

**Acknowledgments.** Support for this work was provided by the NSF (AST-9617185) and by NASA (NAG 5-6399 and HST-GO-08672.01-A), the latter from the Space Telescope Science Institute, which is operated by AURA, Inc., under NASA contract NAS5-26555. N. Bond, J. Rigby, and S. Zonak were supported by an NSF REU Supplement.

**References**

Bahcall, J. N., et al. 1993, *ApJS*, 87, 1

Bahcall, J. N., et al. 1996, *ApJ*, 457, 19

Bergeron, J., & Boissé, P. 1991, *A&A*, 243, 344

Charlton, J. C., Ding, J., Zonak, S. G., Bond, N. A., Churchill, C. W., & Rigby, J. R. 2001, *ApJ*, in preparation

Churchill, C. W., Mellon, R. R., Charlton, J. C., Jannuzi, B. T., Kirhakos, S., & Steidel, C. C., 2000, *ApJS*, 130, 91

Churchill, C. W., Rigby, J. R., Charlton, J. C., & Vogt, S. S. 1999, *ApJS*, 120, 51

Ferland, G. 1996, Hazy, University of Kentucky, Internal Report

Haardt, F., & Madau, P. 1996, *ApJ*, 461, 20

Jannuzi, B. T., et al. 1998, *ApJS*, 118, 1

Rigby, J. R., Charlton, J. C., & Churchill, C. W. 2001, *ApJ*, submitted

Steidel, C. C. 1995, in *QSO Absorption Lines*, ed. G. Meylan (Garching:Springer-Verlag), 139

Steidel, C. C., Dickinson, M. & Persson, E. 1994, *ApJ*, 437, L75

Steidel, C. C., & Sargent, W. L. W. 1992, *ApJS*, 80, 1